Bioorganic & Medicinal Chemistry 20 (2012) 4336–4347

Contents lists available at SciVerse ScienceDirect

Bioorganic & Medicinal Chemistry

journal homepage: www.elsevier.com/locate/bmc

Inhibition of monoamine oxidase by 8-phenoxymethylcaffeine derivatives

Thokozile Okaecwe [a], Abraham J. Swanepoel [a], Anél Petzer [b], Jacobus J. Bergh [a], Jacobus P. Petzer [a,*]

[a] Pharmaceutical Chemistry, School of Pharmacy, North-West University, Private Bag X6001, Potchefstroom 2520, South Africa
[b] Unit for Drug Research and Development, School of Pharmacy, North-West University, Private Bag X6001, Potchefstroom 2520, South Africa

ARTICLE INFO

Article history:
Received 28 March 2012
Revised 11 May 2012
Accepted 17 May 2012
Available online 24 May 2012

Keywords:
Monoamine oxidase
Reversible inhibition
Competitive
Selectivity
Caffeine
Phenoxymethylcaffeine
8-[(Phenylsulfanyl)methyl]caffeine
Molecular docking

ABSTRACT

A recent study has reported that a series of 8-benzyloxycaffeines are potent and reversible inhibitors of both human monoamine oxidase (MAO) isoforms, MAO-A and -B. In an attempt to discover additional caffeine derivatives with potent MAO inhibitory activities, and to contribute to the known structure–activity relationships of MAO inhibition by caffeine derived compounds, the present study investigates the MAO inhibitory potencies of series of 8-phenoxymethylcaffeine and 8-[(phenylsulfanyl)methyl]caffeine derivatives. The results document that the 8-phenoxymethylcaffeine derivatives act as potent reversible inhibitors of MAO-B, with IC_{50} values ranging from 0.148 to 5.78 μM. In contrast, the 8-[(phenylsulfanyl)methyl]caffeine derivatives were found to be weak inhibitors of MAO-B, with IC_{50} values ranging from 4.05 to 124 μM. Neither the 8-phenoxymethylcaffeine nor the 8-[(phenylsulfanyl)methyl]caffeine derivatives exhibited high binding affinities for MAO-A. While less potent than the 8-benzyloxycaffeines as MAO-B inhibitors, this study concludes that 8-phenoxymethylcaffeines may act as useful leads for the design of MAO-B selective inhibitors. Such compounds may find application in the therapy of neurodegenerative disorders such as Parkinson's disease. Using molecular docking experiments, this study also proposes possible binding orientations of selected caffeine derivatives in the active sites of MAO-A and -B.

1. Introduction

The monoamine oxidases (MAO) A and B are apoenzymes, which require flavin adenine dinucleotide (FAD) as cofactor.[1] The MAO enzymes are bound to the outer surface of mitochondria and are expressed in most human tissues, including the brain.[2,3] An important function of the MAOs is to catalyze the oxidative catabolism of neurotransmitters, including serotonin, dopamine and epinephrine, thereby terminating their actions.[4] The MAOs also function as metabolic barriers by restricting the access of extraneous amines to the systemic circulation and the central nervous system. By metabolizing false neurotransmitters such as benzylamine and β-phenylethylamine,[4,5] brain microvessel MAO-B limits their passage into the brain tissue and thus protects neurons from their stimulatory effects.[6] In the gut wall, intestinal MAO-A metabolizes tyramine, an indirectly-acting sympathomimetic amine which is present in certain foods. MAO-A thereby restricts the amount of tyramine that enters the systemic circulation and prevents the tyramine-induced release of catecholamines from peripheral neurons.[7]

Although the amino acid sequences of MAO-A and -B are approximately 73% identical, they exhibit different substrate and inhibitor specificities.[8] Most notably, the MAO-A isoform selectively oxidizes serotonin while MAO-B selectively catalyzes the oxidation of the arylalkylamines, benzylamine and β-phenylethylamine. Both isoforms utilize dopamine, epinephrine and norepinephrine as substrates.[4] The interest in the MAOs as drug targets stems from their roles in the catabolism of these neurotransmitters. MAO-A inhibitors have been employed as antidepressant agents while MAO-B inhibitors have been developed as therapy for Parkinson's disease.[4,9] These clinical applications of MAO-A and -B inhibitors are thought to be, for the most part, dependent on the blocking of the central catabolism of serotonin and dopamine, respectively. In Parkinson's disease therapy, MAO-B inhibitors are frequently combined with levodopa, the metabolic precursor of dopamine.[10] The inhibition of the MAO-B catalyzed oxidation of dopamine in the brain may elevate the levels of dopamine derived from levodopa and may allow for a reduction of the levodopa dose required for a therapeutic effect.[11] MAO-B inhibitors are of particular relevance in Parkinson's disease since MAO-B is the major isoform in the basal ganglia, the affected brain region in Parkinson's disease.[12,13] Furthermore, MAO-B activity and density increases in most brain regions with age while MAO-A activity remains constant.[14,15] This presents a further rationale for targeting MAO-B in age-related neurodegenerative disorders such as Parkinson's disease.[16] Another point of interest is that the MAOs may be major sources of hydrogen peroxide in cells. Following the oxidation of a substrate molecule, the reoxidation of the flavin requires the reduction of molecular

* Corresponding author. Tel.: +27 18 2992206; fax: +27 18 2994243.
E-mail address: jacques.petzer@nwu.ac.za (J.P. Petzer).

0968-0896/$ - see front matter © 2012 Elsevier Ltd. All rights reserved.
http://dx.doi.org/10.1016/j.bmc.2012.05.048

oxygen to yield hydrogen peroxide. Hydrogen peroxide may lead to pathological oxidative stress and promote the neurodegenerative processes associated with Parkinson's disease.[17,18] Also, the aldehydic products, formed as a result of the MAO catalyzed oxidative deamination of amines, may act as neurotoxic metabolites by reacting with exocyclic amino groups of nucleosides, and N-terminal and lysine ε-amino groups of proteins. MAO-B inhibitors may therefore also exert a neuroprotective effect by reducing the formation of these potentially toxic by-products.[1]

Considering the pharmacological importance of MAO inhibitors, the present study aims to discover new inhibitors of the MAOs with particular emphasis on the MAO-B isoform. For this purpose, caffeine derived structures will serve as lead compounds (Fig. 1). Recent studies have reported that 8-benzyloxycaffeines (**1**) act as potent reversible inhibitors of both MAO-A and -B.[19] A homologous series of and 8-sulfanylcaffeines (**2**) has similarly been shown to inhibit MAO-B, and to a lesser degree MAO-A.[20] The 8-benzyloxycaffeines are of particular interest since, unlike most caffeine derived MAO inhibitors, they also possess high binding affinities for MAO-A. The ability of these compounds to also bind to MAO-A may be attributed to the relatively large degree of rotational freedom of the C8 side chain at the carbon–oxygen ether bond. It has been suggested that structures with a relatively larger degree of conformational freedom may be better suited for binding to MAO-A than relatively rigid structures.[19] MAO-A inhibition may also have a role in Parkinson's disease therapy since, in the primate brain, MAO-A also contributes to the catabolism of dopamine.[21] Nonselective MAO-A/B inhibitors may therefore be more efficacious in blocking the oxidation of dopamine and thereby prolonging its effect in the basal ganglia.[1] Based on the promising activities of the 8-benzyloxycaffeines and 8-sulfanylcaffeines, the present study investigates the human MAO inhibitory potencies of series of 8-phenoxymethylcaffeine (**3**) and 8-[(phenylsulfanyl)methyl]caffeine (**4** and **5**) derivatives (Fig. 2). The 8-phenoxymethylcaffeines (**3**) are isomers of **1** while the 8-[(phenylsulfanyl)methyl]caffeines (**4** and **5**) are close structural analogues of **2**. The major difference between the structures of compounds **3**–**5** and that of 8-benzyloxycaffeine is in the placement of the hetero atom in the C8 side chain. In compounds **3**–**5** the position of the hetero atom is distal from the caffeine ring and these compounds are expected to exhibit a differing degree of flexibility than 8-benzyloxycaffeine. Since the degree of flexibility of the 8-benzyloxycaffeine C8 side chain plays an important role in its binding to particularly MAO-A, compounds **3**–**5** may differ in their MAO inhibitory properties compared to the 8-benzyloxycaffeines. The possibility therefore exists that compounds **3**–**5** may display limited inhibition of MAO-A, making them MAO-B selective inhibitors. This study aims to explore this possibility. This study may also contribute to the known structure–activity relationships of MAO inhibition by caffeine derived compounds.

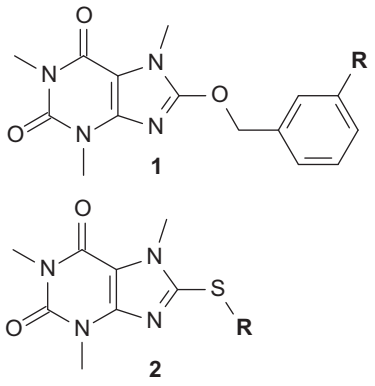

Figure 1. The structures of 8-benzyloxycaffeines (**1**) and 8-sulfanylcaffeines (**2**).

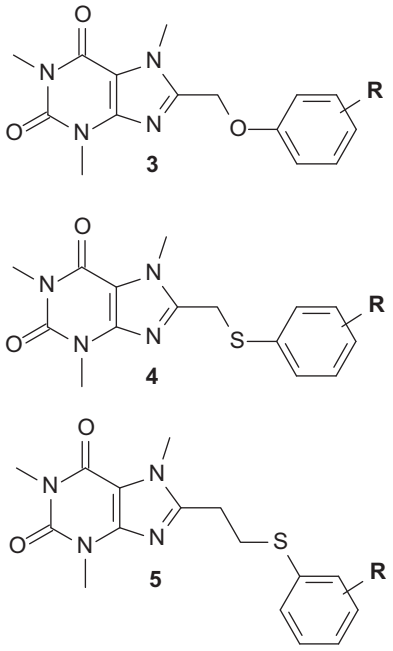

Figure 2. The structures of the 8-phenoxymethylcaffeine (**3**), 8-[(phenylsulfanyl)methyl]caffeine (**4**) and 8-[(phenylsulfanyl)ethyl]caffeine (**5**) derivatives that were investigated in this study.

2. Results

2.1. Chemistry

The syntheses of the 8-phenoxymethylcaffeine derivatives **3a**–**j** were accomplished using the literature procedure (Scheme 1).[22] 1,3-Dimethyl-5,6-diaminouracil (**6**)[23] was allowed to react with the appropriate phenoxyacetic acid (**7**) in the presence of the carbodiimide activating reagent, *N*-(3-dimethylaminopropyl)-*N*′-ethylcarbodiimide hydrochloride (EDAC). The resulting amide

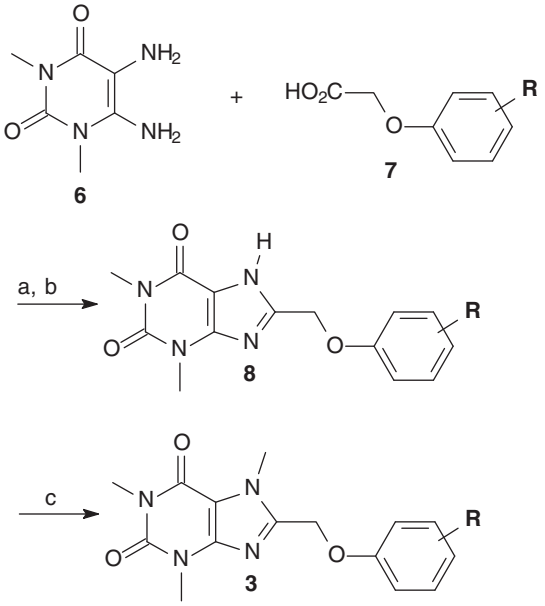

Scheme 1. Synthetic pathway to the 8-phenoxymethylcaffeine derivatives **3**. Reagents and conditions: (a) EDAC dioxane/H_2O, rt; (b) dioxane/NaOH (aq), reflux; (c) CH_3I, K_2CO_3, DMF, 90 °C.

intermediate was treated under reflux with aqueous sodium hydroxide to yield the corresponding 8-phenoxymethyltheophylline intermediate (**8**). Without further purification, the crude theophylline was 7N-methylated with an excess of iodomethane to yield the target compounds, the 8-phenoxymethylcaffeine derivatives **3a**–**j**. The 8-[(phenylsulfanyl)methyl]caffeine derivatives, **4a**–**i** and **5a**–**e**, were prepared in a similar manner by reacting 1,3-dimethyl-5,6-diaminouracil with an appropriate 2-(phenylsulfanyl)acetic acid (**9**) or 3-(phenylsulfanyl)propanoic acid (**10**), respectively (Scheme 2). After ring closure of the resulting amide, the theophylline intermediate (**11**) was obtained. Methylation of **11** in the presence of iodomethane yielded the target 8-[(phenylsulfanyl)methyl]caffeine derivatives **4a**–**i** and **5a**–**e**. Following crystallization, the structures of all compounds were verified by mass spectrometry, ^{1}H NMR and ^{13}C NMR. In certain instances the phenoxyacetic acids (**7**), 2-(phenylsulfanyl)acetic acids (**9**) and 3-(phenylsulfanyl)propanoic acids (**10**), which were required for the synthesis of **3**–**5**, were not commercially available (Table 1). These reagents were thus synthesized according to literature procedures by reacting the appropriate phenol or thiophenol with chloroacetic acid or 3-chloropropionic acid in the presence of base (Scheme 3).[24,25]

2.2. Inhibition studies

The inhibitory potencies of the caffeine derivatives, compounds **3**–**5**, towards MAO were examined by employing recombinant human MAO-A and -B as enzyme sources. Kynuramine, a MAO-A/B mixed substrate, served as substrate for the inhibition studies with both enzymes. The determination of MAO catalytic rates in the presence of compounds **4a**–**i** was accomplished by measuring the concentration of 4-hydroxyquinoline, the MAO catalyzed oxidation product of kynuramine, via fluorescence spectrophotometry.[26] 4-Hydroxyquinoline is a fluorescent compound which is readily measured in the presence of the nonfluorescent kynuramine at excitation and emission wavelengths of 310 nm and 400 nm, respectively. Under these conditions, inhibitors **4a**–**i** do not fluoresce, or quench the fluorescence of 4-hydroxyquinoline. Analogous

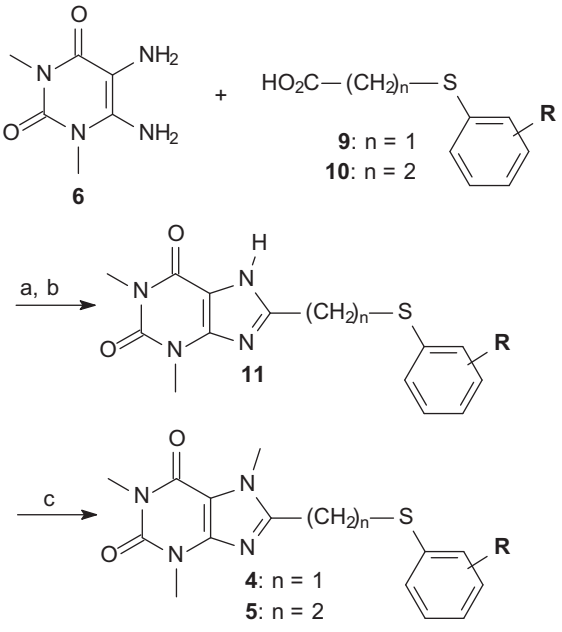

Scheme 2. Synthetic pathway to 8-[(phenylsulfanyl)methyl]caffeines (**4**) and 8-[(phenylsulfanyl)ethyl]caffeines (**5**). Reagents and conditions: (a) EDAC dioxane/H_2O, rt; (b) dioxane/NaOH (aq), reflux; (c) CH_3I, K_2CO_3, DMF, 90 °C.

measurements of 4-hydroxyquinoline concentrations in the presence of inhibitors **3a**–**j** and **5a**–**e** were not possible since these inhibitors fluoresce under the conditions described above, and interfere with the fluorometric determination of 4-hydroxyquinoline at higher inhibitor concentrations. The determination of MAO catalytic rates in the presence of compounds **3a**–**j** and **5a**–**e** was accomplished by measuring the amount of hydrogen peroxide that is produced in the MAO oxidation cycle. In a horseradish peroxidase-coupled reaction, hydrogen peroxide reacts with Ampliflu Red to yield resorufin, a fluorescent compound.[27] Concentration measurement of resorufin may be readily made via fluorescence spectrophotometry at excitation and emission wavelengths of 560 nm and 590 nm, respectively. Under these conditions, inhibitors **3a**–**j** and **5a**–**e** do not fluoresce, or quench the fluorescence of resorufin. The MAO inhibition potencies of the inhibitors are expressed as the IC_{50} values which were estimated from sigmoidal curves of the rate of MAO catalysis versus the logarithm of the inhibitor concentration (Fig. 3).

2.2.1. IC_{50} values for the inhibition of MAO-B

The MAO inhibition potencies of the caffeine derivatives, compounds **3**–**5**, are presented in Tables 2–4. The results show that, among the compounds evaluated, the 8-phenoxymethylcaffeine derivatives, **3a**–**j**, are the most potent inhibitors of MAO-B with IC_{50} values ranging from 0.148 to 5.78 μM. The weakest MAO-B inhibitor among the 8-phenoxymethylcaffeine derivatives is the unsubstituted derivative **3a** (IC_{50} = 5.78 μM). Substitution on the *meta* and *para* positions of the phenyl ring with both halogens (Cl, Br and F) and alkyl groups (CF_3, CH_3, OCH_3) leads to enhanced inhibition. With the exception of **3d**, the *meta* fluorine substituted homologue (IC_{50} = 1.61 μM), halogen containing substituents on the phenyl ring yields compounds with IC_{50} values in the submicromolar range. Bromine substitution on the *meta* (**3c**) and *para* (**3i**) positions was found to be particularly appropriate for MAO-B inhibition and yielded the most potent inhibitors of this study with IC_{50} values of 0.148 μM and 0.189 μM, respectively. These compounds are 30- to 39-fold more potent as MAO-B inhibitors than the unsubstituted homologue **3a**. Compared to halogen substitution, substitution on the *meta* position with the methyl (**3f**, IC_{50} = 1.23 μM) and methoxy (**3g**, IC_{50} = 1.96 μM) groups led to a modest enhancement of the MAO-B inhibition, with these compound being only 3- to 4-fold more potent than **3a**.

The results of the MAO inhibition studies with the 8-[(phenylsulfanyl)methyl]caffeine derivatives, **4a**–**i**, are presented in Table 3. As shown, compounds **4a**–**i** were found to be relatively weak inhibitors of MAO-B with IC_{50} values ranging from 4.05 to 23.4 μM. As observed for the 8-phenoxymethylcaffeine derivatives, the unsubstituted homologue, compound **4a** (IC_{50} = 23.4 μM) was the weakest MAO-B inhibitor of this series, and substitution on the *meta* and *para* positions of the phenyl ring leads to enhanced inhibition. Also similar to the results obtained with the 8-phenoxymethylcaffeine derivatives, *meta* (**4c**) and *para* (**4i**) substitution with bromine yielded the most potent MAO-B inhibitors of this series with IC_{50} values of 4.90 μM and 4.05 μM, respectively. Compared to the bromine substituted 8-phenoxymethylcaffeines (**3c** and **3i**), compounds **4c** and **4i** are, however, 21- to 33-fold weaker as MAO-B inhibitors. This observation leads to the conclusion that phenoxymethylcaffeines are better suited as lead compounds for the design of MAO-B inhibitors than 8-[(phenylsulfanyl)methyl]caffeines. To explore the possibility of improving the MAO inhibition properties of **4a**–**i**, a series of 8-[(phenylsulfanyl)ethyl]caffeine derivatives, **5a**–**e**, were examined as MAO inhibitors. As shown in Table 4, compounds **5a**–**e** proved to be weak MAO-B inhibitors, in most instances weaker than the corresponding 8-[(phenylsulfanyl)methyl]caffeine derivatives (**4**). It may thus be concluded that extending the C8 side chain of 8-[(phenylsulfa-

Table 1
The structures of carboxylic acid derivatives **7**, **9** and **10**

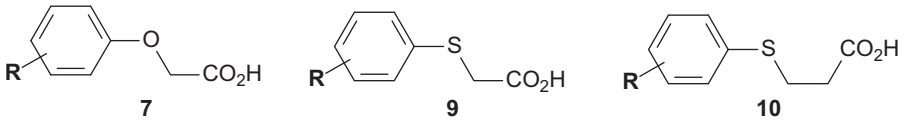

	R	Mp (°C)	Lit. mp (°C)		R	mp (°C)	Lit. mp (°C)
7a	H	Commercially available (98–100)		**9c**	3-Br	90	86.8–87.6[c]
7b	3-Cl	108–109	108–110[a]	**9d**	3-F	74	73.5–74.2[c]
7c	3-Br	107–108	107–108.8[a]	**9e**	3-CH_3	70	66.8–67.4[c]
7d	3-F	114–115	111–112[a]	**9f**	3-OCH_3	72	62.3–63.5[c]
7e	3-CF_3	92–93	93.5–94.5[b]	**9g**	3-OCH_2CH_3	106	New compd
7f	3-CH_3	101–105	102–103.5[a]	**9h**	4-Cl	107	107–108[c]
7g	3-OCH_3	117–118	111–118[a]	**9i**	4-Br	117	118–118.5[c]
7h	4-Cl	Commercially available (157)		**10a**	H	63	58.5–59.5[d]
7i	4-Br	Commercially available (149–153)		**10b**	3-Cl	83	77–78[e]
7j	4-F	Commercially available (104)		**10c**	3-Br	91	90–91[e]
9a	H	Commercially available (60–63)		**10d**	4-Cl	88	90–91[e]
9b	3-Cl	86	81.5–82.2[c]	**10e**	4-Br	116	114–115[e]

[a] Value obtained from Ref. 37.
[b] Value obtained from Ref. 38.
[c] Value obtained from Ref. 39.
[d] Value obtained from Ref. 40.
[e] Value obtained from Ref. 41.

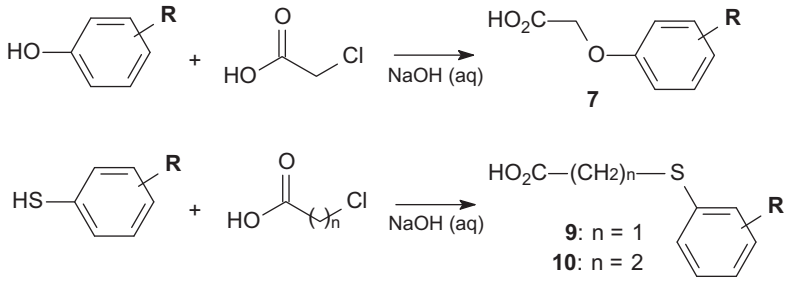

Scheme 3. Synthetic pathway to carboxylic acid derivatives **7**, **9** and **10**.

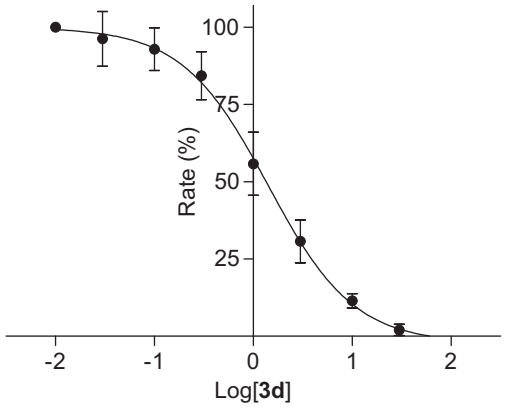

Figure 3. An example sigmoidal dose–response curve of the initial rate of oxidation of kynuramine by recombinant human recombinant human MAO-B versus the logarithm of concentration of an inhibitor (expressed in μM). These determinations were carried out in duplicate and the values are expressed as the mean ± SD.

nyl)methyl]caffeine derivatives does not improve their MAO-B inhibitory potencies.

2.2.2. IC_{50} values for the inhibition of MAO-A

As shown in Table 2, the 8-phenoxymethylcaffeine derivatives, **3a**–**j**, were relatively weak inhibitors of MAO-A, with the most potent inhibitor, compound **3e**, exhibiting an IC_{50} value of 4.59 μM. All of the 8-phenoxymethylcaffeine derivatives were, however, selective for the MAO-B isoform with selectivity indices ranging from 4 to 230. The most selective inhibitor, compound **3c**, also is the most potent MAO-B inhibitor of the compounds investigated. It may thus be concluded that **3c** represents a potent MAO-B selective inhibitor. The 8-[(phenylsulfanyl)methyl]caffeine (**4a**–**i**) and 8-[(phenylsulfanyl)ethyl]caffeine (**5a**–**e**) derivatives were similarly found to be weak MAO-A inhibitors with the most potent homologue, compound **4b**, exhibiting an IC_{50} value of 19.4 μM. Interestingly, **5b** exhibited no MAO-A inhibition, thus making it a highly selective MAO-B inhibitor. This structure may therefore serve as a lead in design studies where absolute selectivity is required.

2.2.3. Reversibility of MAO inhibition

Caffeine derived MAO inhibitors have been shown to interact reversibly with the MAO enzymes.[28] This is a desirable property since de novo synthesis is not required for the recovery of enzyme activity. Enzyme activity is recovered when the inhibitor is cleared from the tissues. Since the 8-phenoxymethylcaffeines may represent a promising new class of MAO inhibitors, this study verified that they interact reversibly with MAO-A and -B. For this purpose the time-dependence of MAO inhibition by 2 selected inhibitors was examined. Compounds **3e** and **3c** were selected as representative inhibitors since they were found to be the most potent inhibitors of MAO-A and -B, respectively, among the 8-phenoxymethylcaffeines.

Table 2
The IC_{50} values for the inhibition of recombinant human MAO-A and -B by compounds **3a–j**

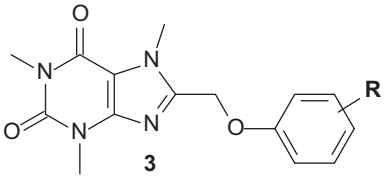

	R	IC_{50}[a,b] (μM)		SI[c]
		MAO-A	MAO-B	
3a	H	21.1 ± 3.23	5.78 ± 0.935	4
3b	3-Cl	No inhibition	0.334 ± 0.010	—
3c	3-Br	34.0 ± 31.5[d]	0.148 ± 0.002	230
3d	3-F	13.2 ± 7.74	1.61 ± 0.723	8
3e	3-CF_3	4.59 ± 1.06	0.641 ± 0.010	7
3f	3-CH_3	18.8 ± 1.52	1.23 ± 0.088	15
3g	3-OCH_3	No inhibition	1.96 ± 0.065	—
3h	4-Cl	20.4 ± 7.27	0.250 ± 0.040	82
3i	4-Br	10.7 ± 2.89	0.189 ± 0.018	57
3j	4-F	8.22 ± 0.336	0.825 ± 0.044	10

[a] All values are expressed as the mean ± SD of duplicate determinations.
[b] The horseradish peroxidase-coupled reaction with Ampliflu Red was used to measure MAO activities.
[c] The selectivity index is the selectivity for the MAO-B isoform and is given as the ratio of IC_{50}(MAO-A)/IC_{50}(MAO-B).
[d] Limited solubility restricts the determination of an accurate IC_{50} value.

Table 3
The IC_{50} values for the inhibition of recombinant human MAO-A and -B by compounds **4a–i**

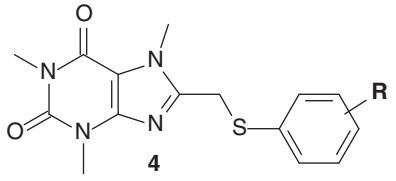

	R	IC_{50}[a,b] (μM)		SI[c]
		MAO-A	MAO-B	
4a	H	66.2 ± 5.32	23.4 ± 9.83	3
4b	3-Cl	19.4 ± 0.35	6.12 ± 0.45	3
4c	3-Br	23.8 ± 0.95	4.90 ± 1.04	5
4d	3-F	50.1 ± 1.84	22.3 ± 3.82	2
4e	3-CH_3	51.8 ± 4.20	17.9 ± 0.99	3
4f	3-OCH_3	41.3 ± 2.56	8.42 ± 0.10	5
4g	3-OCH_2CH_3	44.7 ± 2.29	18.4 ± 0.70	2
4h	4-Cl	31.6 ± 0.54	6.91 ± 0.65	5
4i	4-Br	20.8 ± 1.62	4.05 ± 0.77	5

[a] All values are expressed as the mean ± SD of triplicate determinations.
[b] MAO activities were determined by measuring 4-hydroxyquinoline formation via fluorescence spectrophotometry.
[c] The selectivity index is the selectivity for the MAO-B isoform and is given as the ratio of IC_{50}(MAO-A)/IC_{50}(MAO-B).

These inhibitors were preincubated with MAO-A or -B for time periods of 0, 15, 30 and 60 min. These preincubations were conducted at inhibitor concentrations of approximately twofold their measured IC_{50} values for the inhibition of the respective MAO enzymes. Following these preincubations the reactions were diluted twofold, to yield inhibitor concentrations equal to their IC_{50} values, and the residual MAO catalytic activities were measured. The results of these reversibility studies are shown in Figure 4. When **3e** and **3c** were

Table 4
The IC_{50} values for the inhibition of recombinant human MAO-A and -B by compounds **5a–e**

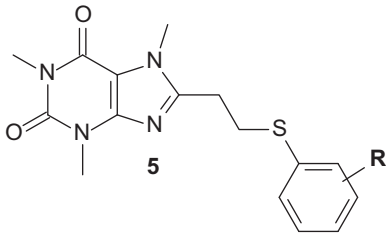

	R	IC_{50}[a,b] (μM)		SI[c]
		MAO-A	MAO-B	
5a	H	139 ± 8.82	108 ± 32.7	1.3
5b	3-Cl	No inhibition	5.67 ± 3.55	—
5c	3-Br	372 ± 121	64.1 ± 9.73	6
5d	4-Cl	142 ± 40.6	7.79 ± 0.66	18
5e	4-Br	117 ± 13.7	124 ± 14.2	0.9

[a] All values are expressed as the mean ± SD of triplicate determinations.
[b] The horseradish peroxidase-coupled reaction with Ampliflu Red was used to measure MAO activities.
[c] The selectivity index is the selectivity for the MAO-B isoform and is given as the ratio of IC_{50}(MAO-A)/IC_{50}(MAO-B).

preincubated with MAO-A and -B, respectively, no time-dependent reductions of the catalytic activities occurred, even following a period of 60 min preincubation with the enzyme. These data are consistent with a reversible interaction of **3e** and **3c** with MAO-A and -B, respectively.

To provide further evidence for the reversible interaction of 8-phenoxymethylcaffeines with MAO, Lineweaver–Burk plots were constructed for the inhibition of MAO-B by compound **3c**. The MAO-B catalytic rates were measured in the absence of inhibitor, and presence of three different concentrations of **3c**. These measurements were carried out using four different concentrations of the substrate, kynuramine (15–90 μM). A set of 4 Lineweaver–Burk plots were constructed from these experiments and is given in Figure 5. The results show that the Lineweaver–Burk plots are linear and intersect at the *y*-axis. This indicates that the inhibition of MAO-B by **3c** is competitive, and is further support that **3c** is a reversible MAO-B inhibitor.

2.2.4. Modelling studies

The results of the MAO inhibition studies have shown that **3c** acts as a potent MAO-B inhibitor while its sulfanyl homologue, compound **4c**, is approximately 33-fold less potent as an MAO-B inhibitor. Also, **3c** is a highly selective inhibitor of MAO-B, with a 230-fold selectivity over the MAO-A isoform. To provide additional insight, possible binding orientations of **3c** and **4c** within the MAO active sites were explored. For this purpose, molecular docking with the CDOCKER module of Discovery Studio 3.1 (Accelrys)[29] was carried out. The crystallographic structures of human MAO-A cocrystallized with harmine (PDB entry: 2Z5X)[30] and human MAO-B cocrystallized with 7-(3-chlorobenzyloxy)-4-formylcoumarin (PDB entry: 2V60)[31] served as protein models. These protein models and docking protocol have previously been shown to be appropriate for predicting binding orientations of ligands in the active sites of MAO-A and -B.[32]

The highest ranked solution of **3c** within the MAO-B active site is illustrated in Figure 6. The orientations of the ten best solutions differed by less than 0.08 Å from the highest ranked solution. As shown, the caffeine ring of the inhibitor binds within the substrate cavity of the enzyme, in proximity to the FAD cofactor. In the space directly in front of the FAD cofactor, which is considered to be the

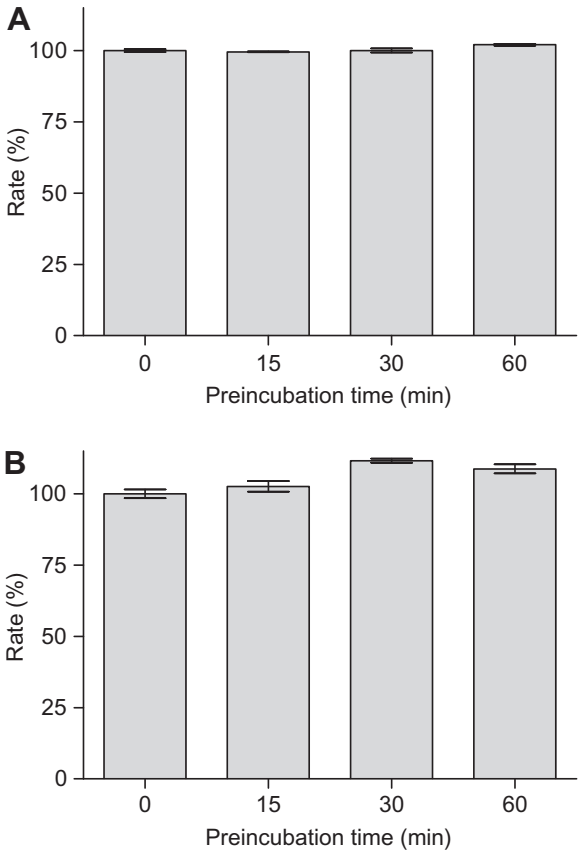

Figure 4. Time-dependant inhibition of recombinant human MAO-A (Panel A) and recombinant human MAO-B (Panel B) by **3e** and **3c**, respectively. The enzymes were preincubated for various periods of time (0–60 min) with **3e** (MAO-A) and **3c** (MAO-B) at inhibitor concentrations of 9.7 μM and 0.3 μM, respectively.

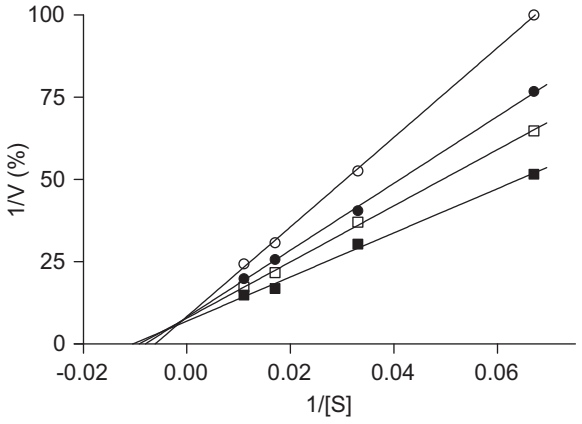

Figure 5. Lineweaver–Burk plots of the recombinant human MAO-B catalyzed oxidation of kynuramine in the absence (filled squares) and presence of various concentrations of **3c**. The concentrations employed for **3c** were 0.0375 μM (open squares), 0.075 μM (filled circles), 0.15 μM (open circles).

polar part of the active site, the C6 carbonyl oxygen of the caffeine ring undergoes potential hydrogen bonding with the phenolic hydrogen of Tyr-435 and a water molecule. Furthermore, the caffeine ring is orientated approximately parallel to the phenyl rings of Tyr-435 and Tyr-398, an orientation that is restricted by the flat shape of the substrate cavity. This places the caffeine ring within π–π interaction distance to Tyr-398. The C8 phenoxymethyl side chain of **3c** extends into the entrance cavity of MAO-B. Since the entrance cavity constitutes a highly hydrophobic environment, the C8 substituents are expected to be stabilized principally by Van der Waals interactions within this space.[33] An analysis of the interaction energies suggests particular favorable Van der Waals interactions with Ile-199 and Leu-171. Figure 7 illustrates the highest ranked solution of **4c** within the MAO-B active site. In this instance, the orientations of the ten best solutions differed by less than 0.07 Å from the highest ranked solution. Compound **4c** exhibits a similar orientation with respect to the placement of the caffeine ring and C8 side chain to that observed for **3c**. The most notable difference, however, is that the polar functional groups of the caffeine ring of **4c** are not placed within hydrogen bond interaction distance to residues and waters in the substrate cavity. Calculation of the interaction energies show that an unfavorable interaction may exist between the thioether sulfur of **4c** and Tyr-326. This interaction is most likely due to close contact between these moieties. This unfavorable interaction with Tyr-326 and the loss of potential hydrogen bonding may explain the reduced binding affinity of **4c** for the MAO-B active site compared **3c**.

The highest ranked docking orientation of **3c** within the MAO-A active site is presented in Figure 8. Similar to its orientation in MAO-B, compound **3c** binds with the caffeine ring in the proximity of the FAD cofactor while the C8 phenoxymethyl side chain extends towards the entrance of the MAO-A active site. The inhibitor may undergo π–π and π–σ interactions with Tyr-407 and Phe-208, respectively, as well as hydrogen bonding with an active site water molecule. The most notable difference between the binding orientations of **3c** in MAO-A and -B is that, in MAO-A, **3c** binds in a folded conformation, while exhibiting an extended conformation in the MAO-B active site. The folded conformation observed in the MAO-A active site is, to a large degree, imposed by the bulk of the phenyl side chain of Phe-208. This residue may impede the binding of relatively large inhibitors in the MAO-A active site, and, in order to avoid structural overlap with Phe-208, larger inhibitors adopt a folded conformation. In the MAO-B active site, the residue occupying the analogous position to Phe-208 is Ile-199. The side chain of Ile-199, which is comparatively smaller compared to the phenyl ring of Phe-208, is able to rotate from the MAO-B active site cavity, which enables larger inhibitors to bind in an extended

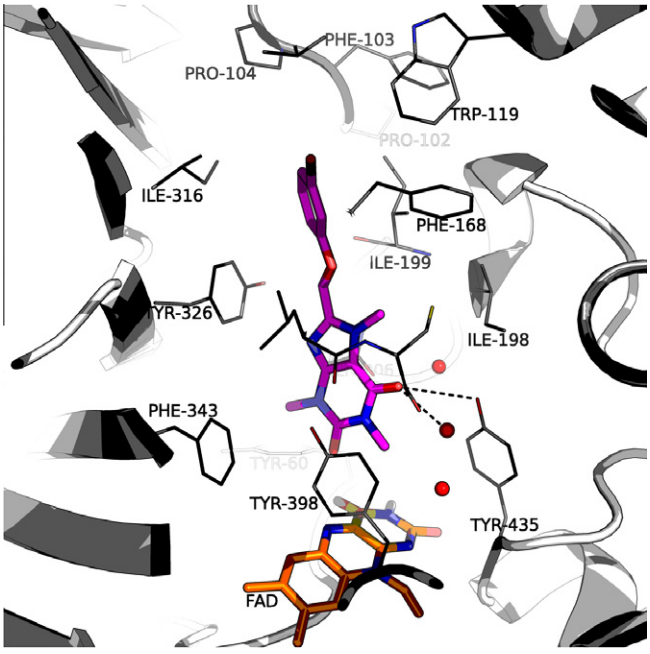

Figure 6. The predicted binding orientation of **3c** within the MAO-B active site.

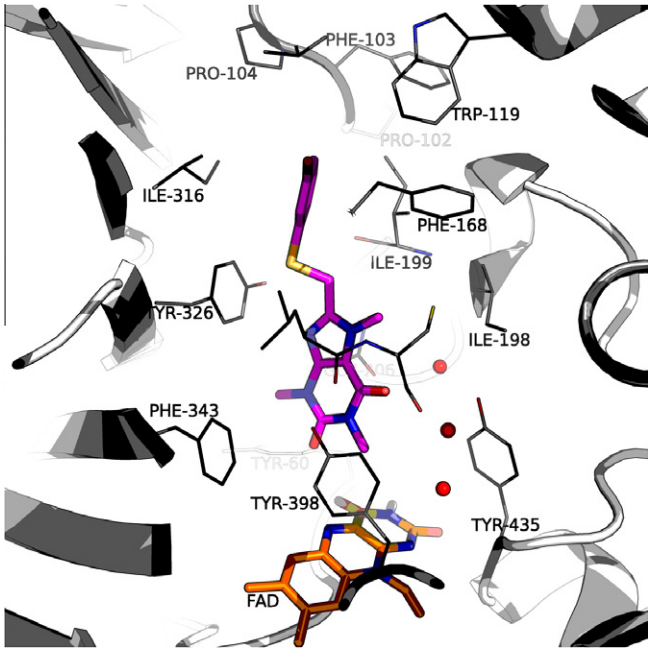

Figure 7. The predicted binding orientation of **4c** within the MAO-B active site.

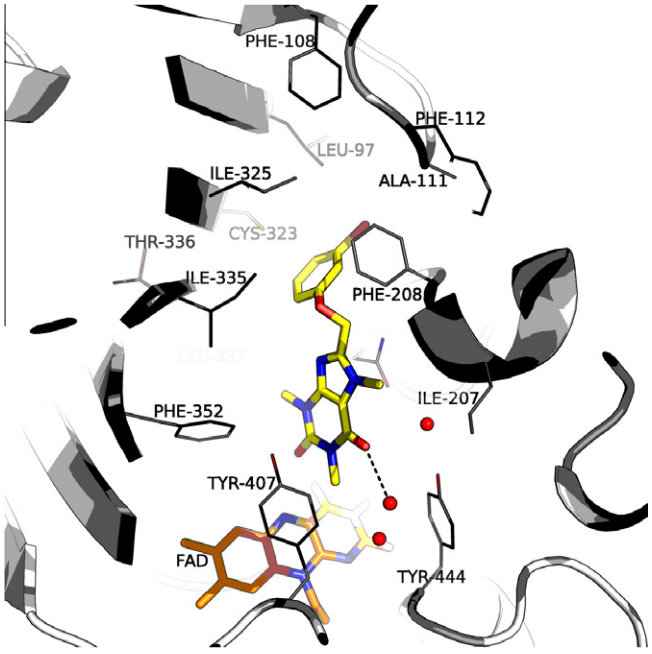

Figure 8. The predicted binding orientation of **3c** within the MAO-A active site.

conformation in MAO-B.[16] An analysis of the interaction energies suggests that the binding orientation of **3c** in MAO-A imposes an unfavorable interaction between the N7 methyl group of the inhibitor and the side chain of Asn-181. Since the extended conformation results in no unfavorable interactions with the MAO-B active site, the ability of **3c** to bind in an extended conformation to MAO-B may explain its higher binding affinity for MAO-B. Also, the extended conformation may allow for more and improved productive interactions between the inhibitor and enzyme than the folded inhibitor conformation.

3. Discussion and conclusion

The present study examines the possibility that series of 8-phenoxymethylcaffeine (**3**) and 8-[(phenylsulfanyl)methyl]caffeine (**4** and **5**) derivatives may act as inhibitors of human MAO. The results demonstrate that the 8-phenoxymethylcaffeines are the most active MAO inhibitors, with 6 compounds exhibiting IC_{50} values in the submicromolar range. The most potent inhibitor, compound **3c**, was also shown to interact reversible and competitively with MAO-B. In contrast, the phenylsulfanyl derivatives **4** and **5** proved to be comparatively weak MAO-B inhibitors. Modelling studies suggest that, while homologues **3c** and **4c** exhibit similar binding orientations in the MAO-B active site, an unfavorable Van der Waals interaction between the thioether sulfur of **4c** and Tyr-326 may explain, in part, the low MAO-B inhibition potency of this inhibitor compared to **3c**. It may therefore be concluded that the 8-phenoxymethylcaffeines, particularly compound **3c**, represent promising lead compounds for the development of reversible MAO-B selective inhibitors. The results obtained with compounds **4** and **5** show that differing substitution on the phenyl ring and modification of the linker between the caffeine and phenyl ring do not improve the MAO inhibitory properties of the 8-[(phenylsulfanyl)methyl]caffeines. Considering these results, it is apparent that 8-[(phenylsulfanyl)methyl]caffeines are not suitable leads for the design of MAO-B inhibitors, and minor structural modifications would not lead to improved inhibitory properties.

Compared with the previously reported 8-benzyloxycaffeines (**1**)[19] the 8-phenoxymethylcaffeines **3** are, however, weaker MAO-B inhibitors. For example, 8-(3-bromobenzyloxy)caffeine, the benzyloxycaffeine homologue of **3c**, inhibits human MAO-B with an IC_{50} value of 0.068 μM, which is approximately twofold more potent than the inhibition potency of **3c**. This result suggests that, the placement of the ether oxygen in the C8 side chain of caffeine derived inhibitors is an important consideration in the design of MAO-B inhibitors. When comparing the MAO-B inhibition potencies of previously reported 8-(benzylsulfanyl)caffeines (**2**)[20] with the potencies of the 8-[(phenylsulfanyl)methyl]caffeine derivatives **4**, a similar conclusion may be drawn. For example, 8-(benzylsulfanyl)caffeines inhibit human MAO-B with IC_{50} values as low as 0.167 μM, while the most potent 8-[(phenylsulfanyl)methyl]caffeine derivative examined here, compound **4i**, inhibits MAO-B with an IC_{50} value of 4.05 μM. Therefore, the position of the thioether sulfur in the C8 side chain of caffeine derived inhibitors also has large effects on the MAO-B inhibition potencies. These results demonstrate that, when a heteroatom is introduced into the C8 side chain of caffeine derived structures, substitution directly on C8 of the caffeine ring is likely to lead to the most potent MAO-B inhibition.

Interestingly, compared to the previously reported 8-benzyloxycaffeines (**1**) the 8-phenoxymethylcaffeine (**3**) exhibited weak inhibition potencies towards MAO-A. As mentioned in Section 1, the ability of 8-benzyloxycaffeines to bind within the MAO-A active site may be attributed to the relatively large degree of rotational freedom of the C8 side chain at the carbon–oxygen ether bond.[19] This rotational freedom presumably enables the inhibitor to adopt the folded conformation required for binding to MAO-A. Although, the 8-phenoxymethylcaffeines also contain a carbon–oxygen ether bond in the C8 side chain, they exhibit weak binding to the MAO-A active site. The position of the ether oxygen in the C8 side chain of caffeine derived inhibitors therefore, in part, determines the affinities of these inhibitor for MAO-A. One potential reason for this observation is that the placement of the ether oxygen distal from the caffeine ring does not allow for the correct measure of flexibility of the C8 side chain for the inhibitor to be accommodated well in the MAO-A binding site. This reduced/modified degree of flexibility may, in part, be accounted for by

differences in the resonance of the phenoxy and the oxycaffeinyl systems.

4. Experimental section

4.1. Chemicals and instrumentation

Unless otherwise noted, all starting materials were obtained from Sigma–Aldrich and were used without further purification. 1,3-Dimethyl-5,6-diaminouracil (**6**) was prepared according to the literature procedure.[23] Proton (^{1}H) and carbon (^{13}C) NMR spectra were recorded on a Bruker Avance III 600 spectrometer at frequencies of 600 MHz and 150 MHz, respectively. All NMR measurements were conducted in $CDCl_3$ and the chemical shifts are reported in parts per million (δ) downfield from the signal of tetramethylsilane. Spin multiplicities are given as s (singlet), br s (broad singlet), d (doublet), dd (doublet of doublets), t (triplet), q (quartet) or m (multiplet). High resolution mass spectra (HRMS) were obtained on a DFS high resolution magnetic sector mass spectrometer (Thermo Electron Corporation) in electron ionization (EI) mode. Melting points (mp) were determined on a Buchi M-545 melting point apparatus and are uncorrected. For fluorescence spectrophotometry, a Varian Cary Eclipse fluorescence spectrophotometer was employed. The following chemical and biological agents were obtained from Sigma–Aldrich: microsomes from insect cells containing recombinant human MAO-A or MAO-B (5 mg/mL), kynuramine·2HBr, Ampliflu Red (10-acetyl-3,7-dihydroxyphenoxazine), horseradish peroxidase, (*R*)-deprenyl·HCl, clorgyline·HCl and H_2O_2 (3%).

4.2. Synthesis of 8-phenoxymethylcaffeine derivatives (3a–j)

The syntheses of **3a**–**j** were accomplished using the literature procedure.[22] 1,3-Dimethyl-5,6-diaminouracil[23] (4 mmol) and *N*-(3-dimethylaminopropyl)-*N*′-ethylcarbodiimide hydrochloride (EDAC; 5.36 mmol) were dissolved in 42 mL dioxane/H_2O (1:1) and the appropriate phenoxyacetic acid (4 mmol) was added. A thick suspension was obtained and the pH was adjusted to 5–6 with 4 N aqueous HCl. The reaction was stirred for 2 h at room temperature and neutralized with aqueous NaOH (1 N). The precipitate was collected by filtration and subsequently dissolved in 40 mL dioxane/H_2O (1:1). The reaction was heated under reflux for 2 h, cooled to 0 °C and acidified to a pH of 4 with 4 N aqueous HCl. The resulting precipitate, the corresponding 1,3-dimethyl-8-substituted-7*H*-xanthinyl analogue, was collected by filtration, washed with 50 mL H_2O and dried at 50 °C. The 7*H*-xanthinyl analogue was used in the subsequent reaction without further purification. The corresponding 1,3-dimethyl-8-substituted-7*H*-xanthinyl analogue (2 mmol) was dissolved in a minimum amount of DMF (approximately 20 mL) at 90 °C. K_2CO_3 (5 mmol), followed by iodomethane (4 mmol), and the reaction mixture was stirred at 90 °C for 1 h. The reaction progress was followed with TLC employing neutral alumina sheets and ethyl acetate/dichloromethane (1:1) as mobile phase. The insoluble materials were removed by filtration. H_2O (350 ml) was added to the filtrate and the mixture was cooled on ice for 3 h. The precipitate that formed was collected by filtration and dried overnight at room temperature. The products were recrystallized from methanol/ethyl acetate (7:5).

4.2.1. 8-Phenoxymethylcaffeine (3a)

The title compound was prepared from phenoxyacetic acid in a yield of 73%: mp 197–199 °C (methanol/ethyl acetate 7:5). ^{1}H NMR ($CDCl_3$) δ 3.37 (s, 3H), 3.56 (s, 3H), 4.03 (s, 3H), 5.17 (s, 2H), 6.99 (m, 3H), 7.29 (t, 2H, J = 7.53 Hz); ^{13}C NMR ($CDCl_3$) δ 27.9, 29.7, 32.4, 62.0, 108.7, 114.6, 122.0, 129.7, 147.4, 147.9, 151.6, 155.4, 157.5; EIMS 300; EI-HRMS m/z: calcd for $C_{15}H_{16}O_3N_4$, 300.1222, found 300.1218.

4.2.2. 8-(3-Chlorophenoxymethyl)caffeine (3b)

The title compound was prepared from 3-chlorophenoxyacetic acid in a yield of 83%: mp 201–203 °C (methanol/ethyl acetate 7:5). ^{1}H NMR ($CDCl_3$) δ 3.38 (s, 3H), 3.56 (s, 3H), 4.02 (s, 3H), 5.15 (s, 2H), 6.87 (dd, 1H, J = 2.6, 8.3 Hz), 6.97 (m, 1H), 7.01 (t, 1H, J = 2.3 Hz), 7.20 (t, 1H, J = 8.3 Hz); ^{13}C NMR ($CDCl_3$) δ 27.9, 29.7, 32.4, 62.1, 108.8, 113.0, 115.4, 122.3, 130.5, 135.1, 147.2, 147.4, 151.5, 155.4, 158.2; EI-HRMS m/z: calcd for $C_{15}H_{15}O_3N_4Cl$, 334.0833, found 334.0843.

4.2.3. 8-(3-Bromophenoxymethyl)caffeine (3c)

The title compound was prepared from 3-bromophenoxyacetic acid in a yield of 78%: mp 200–204 °C (methanol/ethyl acetate 7:5). ^{1}H NMR ($CDCl_3$) δ 3.36 (s, 3H), 3.55 (s, 3H), 4.01 (s, 3H), 5.14 (s, 2H), 6.91 (d, 1H, J = 7.5 Hz), 7.12 (m, 3H); ^{13}C NMR ($CDCl_3$) δ 28.0, 29.7, 32.4, 62.1, 108.8, 113.5, 118.2, 123.0, 125.2, 130.8, 147.2, 147.4, 151.5, 155.4, 158.2; EI-HRMS m/z: calcd for $C_{15}H_{15}O_3N_4Br$, 378.0328, found 378.0301.

4.2.4. 8-(3-Fluorophenoxymethyl)caffeine (3d)

The title compound was prepared from 3-fluorophenoxyacetic acid in a yield of 67%: mp 198–201 °C (methanol/ethyl acetate 7:5). ^{1}H NMR ($CDCl_3$) δ 3.36 (s, 3H), 3.55 (s, 3H), 4.02 (s, 3H), 5.15 (s, 2H), 6.71 (m, 2H), 6.76 (dd, 1H, J = 2.3, 8.3 Hz), 7.22 (m, 1H); ^{13}C NMR ($CDCl_3$) δ 28.0, 29.7, 32.4, 62.2, 102.7 (d), 108.8, 108.9 (d), 110.3 (d), 130.5 (d), 147.3 (d), 151.6, 155.4, 158.7 (d), 162.7, 164.3; EI-HRMS m/z: calcd for $C_{15}H_{15}O_3N_4F$, 318.1128, found 318.1131.

4.2.5. 8-[3-(Trifluoromethyl)phenoxymethyl]caffeine (3e)

The title compound was prepared from 2-[3-(trifluoromethyl)phenoxy]acetic acid in a yield of 52%: mp 172–174 °C (methanol/ethyl acetate 7:5). ^{1}H NMR ($CDCl_3$) δ 3.38 (s, 3H), 3.56 (s, 3H), 4.04 (s, 3H), 5.22 (s, 2H), 7.17 (m, 1H), 7.25 (d, 1H, J = 7.5 Hz), 7.29 (s, 1H), 7.40 (t, 1H, J = 8.3 Hz); ^{13}C NMR ($CDCl_3$) δ 28.0, 29.7, 32.4, 62.1, 108.8, 111.7 (q), 118.2, 118.7 (q), 122.8, 124.6, 130.3, 132.2 (q), 147.0, 147.4, 151.5, 155.4, 157.6; EI-HRMS m/z: calcd for $C_{16}H_{15}O_3N_4F_3$, 368.1096, found 368.1081.

4.2.6. 8-(3-Methylphenoxymethyl)caffeine (3f)

The title compound was prepared from 3-methylphenoxyacetic acid in a yield of 72%: mp 195–196 °C (methanol/ethyl acetate 7:5). ^{1}H NMR ($CDCl_3$) ^{1}H NMR (Bruker Avance III 600, $CDCl_3$) δ 2.30 (s, 3H), 3.70 (s, 3H), 3.55 (s, 3H), 4.02 (s, 3H), 5.14 (s, 2H), 6.80 (m, 3H), 7.16 (t, 1H, J = 8.3 Hz); ^{13}C NMR ($CDCl_3$) δ 21.4, 27.9, 29.7, 32.4, 61.9, 108.7, 111.3, 115.5, 122.8, 129.4, 139.8, 147.3, 148.0, 151.5, 155.4, 157.5; EI-HRMS m/z: calcd for $C_{16}H_{18}O_3N_4$, 314.1379, found 314.1386.

4.2.7. 8-(3-Methoxyphenoxymethyl)caffeine (3g)

The title compound was prepared from 3-methoxyphenoxyacetic acid in a yield of 36%: mp 165–167 °C (methanol/ethyl acetate 7:5). ^{1}H NMR ($CDCl_3$) δ 3.36 (s, 3H), 3.54 (s, 3H), 3.75 (s, 3H), 4.01 (s, 3H), 5.14 (s, 2H), 6.53 (m, 2H), 6.56 (m, 1H), 7.17 (t, 1H, J = 8.7 Hz); ^{13}C NMR ($CDCl_3$) δ 27.9, 29.7, 32.4, 55.3, 62.0, 101.2, 106.6, 107.5, 108.7, 130.1, 147.3, 147.8, 151.5, 155.4, 158.7, 160.9; EI-HRMS m/z: calcd for $C_{16}H_{18}O_4N_4$, 330.1328, found 330.1320.

4.2.8. 8-(4-Chlorophenoxymethyl)caffeine (3h)

The title compound was prepared from 4-chlorophenoxyacetic acid in a yield of 52%: mp 181–183 °C (methanol/ethyl acetate 7:5). ^{1}H NMR ($CDCl_3$) δ 3.36 (s, 3H), 3.54 (s, 3H), 4.01 (s, 3H),

5.13 (s, 2H), 6.91 (d, 2H, J = 8.7 Hz), 7.22 (d, 2H, J = 8.7 Hz); ^{13}C NMR ($CDCl_3$) δ 27.9, 29.7, 32.4, 62.2, 108.7, 116.0, 127.0, 129.6, 147.3, 147.4, 151.5, 155.4, 156.0; EI-HRMS m/z: calcd for $C_{15}H_{15}O_3N_4Cl$, 334.0833, found 334.0838.

4.2.9. 8-(4-Bromophenoxymethyl)caffeine (3i)

The title compound was prepared from 4-bromophenoxyacetic acid in a yield of 80%: mp 195–197 °C (methanol/ethyl acetate 7:5). ^{1}H NMR ($CDCl_3$) δ 3.35 (s, 3H), 3.53 (s, 3H), 4.00 (s, 3H), 5.13 (s, 2H), 6.86 (d, 2H, J = 9.0 Hz), 7.35 (d, 2H, J = 9.0 Hz); ^{13}C NMR ($CDCl_3$) δ 27.9, 29.7, 32.4, 62.1, 108.7, 114.3, 116.4, 132.5, 147.3, 151.5, 155.3, 156.5; EI-HRMS m/z: calcd for $C_{15}H_{15}O_3N_4Br$, 378.0328, found 378.0317.

4.2.10. 8-(4-Fluorophenoxymethyl)caffeine (3j)

The title compound was prepared from 4-fluorophenoxyacetic acid in a yield of 79%: mp 212–213 °C (methanol/ethyl acetate 7:5). ^{1}H NMR ($CDCl_3$) δ 3.37 (s, 3H), 3.55 (s, 3H), 4.02 (s, 3H), 5.13 (s, 2H), 6.94 (m, 4H); ^{13}C NMR ($CDCl_3$) δ 27.9, 29.7, 32.4, 62.6, 108.7, 115.8, 115.9, 116.0, 116.2, 147.3, 147.6, 151.5, 153.6, 155.4, 157.1, 158.7; EI-HRMS m/z: calcd for $C_{15}H_{15}O_3N_4F$, 318.1128, found 318.1114.

4.3. Synthesis of 8-[(phenylsulfanyl)methyl]caffeine (4a–i)

Compounds **4a**–**i** were synthesized from 1,3-dimethyl-5,6-diaminouracil[23] and an appropriate 2-(phenylsulfanyl)acetic acid according to the procedure described above for the syntheses of **3a**–**j**.[22]

4.3.1. 8-[(Phenylsulfanyl)methyl]caffeine (4a)

The title compound was prepared from 2-(phenylsulfanyl)acetic acid in a yield of 74%: mp 154–156 °C (methanol/ethylacetate 7:2). ^{1}H NMR ($CDCl_3$) δ 3.34 (s, 3H), 3.47 (s, 3H), 3.78 (s, 3H), 4.13 (s, 2H), 7.24 (m, 3H), 7.35 (m, 2H); ^{13}C NMR ($CDCl_3$) δ 27.8, 29.6, 30.8, 32.0, 107.9, 128.0, 129.1, 131.9, 133.3, 147.5, 149.4, 151.5, 155.2; EI-HRMS m/z: calcd for $C_{15}H_{16}N_4O_2S$, 316.0994, found 316.0988.

4.3.2. 8-{[(3-Chlorophenyl)sulfanyl]methyl}caffeine (4b)

The title compound was prepared from 2-[(3-chlorophenyl)sulfanyl]acetic acid in a yield of 56%: mp 174–177 °C (methanol/ethylacetate 7:2). ^{1}H NMR ($CDCl_3$) δ 3.35 (s, 3H), 3.49 (s, 3H), 3.90 (s, 3H), 4.17 (s, 2H), 7.19 (m, 2H), 7.23 (m, 1H), 7.41 (m, 1H); ^{13}C NMR ($CDCl_3$) δ 27.9, 29.6, 30.1, 32.1, 108.1, 127.7, 128.9, 130.1, 130.6, 134.7, 135.5, 147.4, 148.8, 151.5, 155.2; EI-HRMS m/z: calcd for $C_{15}H_{15}ClN_4O_2S$, 350.0604, found 350.0615.

4.3.3. 8-{[(3-Bromophenyl)sulfanyl]methyl}caffeine (4c)

The title compound was prepared from 2-[(3-bromophenyl)sulfanyl]acetic acid in a yield of 75%: mp 151–152 °C (methanol/ethylacetate 7:2). ^{1}H NMR ($CDCl_3$) δ, 3.35 (s, 3H), 3.49 (s, 3H), 3.89 (s, 3H), 4.16 (s, 2H), 7.12 (t, 1H, J = 7.9 Hz), 7.27 (m, 1H), 7.34 (m, 1H), 7.56 (m, 1H); ^{13}C NMR ($CDCl_3$) δ 27.9, 29.6, 30.1, 32.1, 108.1, 122.8, 129.4, 130.3, 130.6, 133.4, 135.8, 147.4, 148.8, 151.5, 155.2; EI-HRMS m/z: calcd for $C_{15}H_{15}BrN_4O_2S$, 394.0099, found 394.0100.

4.3.4. 8-{[(3-Flourophenyl)sulfanyl]methyl}caffeine (4d)

The title compound was prepared from 2-[(3-flourophenyl)sulfanyl]acetic acid in a yield of 30%: mp 155–156 °C (methanol/ethylacetate 7:2). ^{1}H NMR ($CDCl_3$) δ, 3.45 (s, 3H), 3.48 (s, 3H), 3.89 (s, 3H), 4.18 (s, 2H), 6.92 (m, 1H), 7.13 (m, 2H), 7.22 (m, 1H); ^{13}C NMR ($CDCl_3$) δ; 27.9, 29.6, 30.1, 32.1, 108.1, 114.5. 114.6, 117.5, 117.6, 126.3, 130.3, 130.4, 135.8, 135.9, 147.4, 148.8, 151.5, 155.2, 161.8, 163.4; EI-HRMS m/z: calcd for $C_{15}H_{15}FN_4O_2S$, 334.0900, found 334.0893.

4.3.5. 8-{[(3-Methylphenyl)sulfanyl]methyl}caffeine (4e)

The title compound was prepared from 2-[(3-methylphenyl)sulfanyl]acetic acid in a yield of 37%: mp 124–126 °C (methanol/ethylacetate 7:2). ^{1}H NMR ($CDCl_3$) δ, 2.32 (s, 3H), 3.39 (s, 3H), 3.53 (s, 3H) 3.85 (s, 3H), 4.18 (s, 2H), 7.09 (br s, 1H), 7.19 (m, 2H), 7.24 (m, 1H); ^{13}C NMR ($CDCl_3$) δ; 21.2, 27.8, 29.6, 30.7, 32.0, 107.9, 128.6, 128.7, 128.9, 132.3, 133.1, 139.0, 147.5, 149.5, 151.5, 155.2; EI-HRMS m/z: calcd for $C_{16}H_{18}N_4O_2S$, 330.1150, found 330.1157.

4.3.6. 8-{[(3-Methoxyphenyl)sulfanyl]methyl}caffeine (4f)

The title compound was prepared from 2-[(3-methoxyphenyl)sulfanyl]acetic acid in a yield of 41%: mp 161–165 °C (methanol/ethylacetate 7:2). ^{1}H NMR ($CDCl_3$) δ; 3.36 (s, 3H), 3.50 (s, 3H), 3.75 (s, 3H), 3.84 (s, 3H), 4.16 (s, 2H), 6.78 (dd, 1H, J = 1.9, 7.9 Hz), 6.93 (m, 2H), 7.17 (t, 1H, J = 7.9 Hz); ^{13}C NMR ($CDCl_3$) δ; 27.9, 29.7, 30.5, 32.1, 55.3, 108.0, 113.6, 116.5, 123.3, 130.0, 134.8, 147.5, 149.4, 151.5, 155.2, 159.9; EI-HRMS m/z: calcd for $C_{16}H_{18}N_4O_3S$, 346.1100, found 346.1091.

4.3.7. 8-{[(3-Ethoxyphenyl)sulfanyl]methyl}caffeine (4g)

The title compound was prepared from 2-[(3-ethoxyphenyl)sulfanyl]acetic acid in a yield of 55%: mp 147–149 °C (methanol/ethylacetate 7:2). ^{1}H NMR ($CDCl_3$) δ 1.35 (t, 3H, J = 6.8 Hz), 3.34 (s, 3H), 3.48 (s, 3H), 3.82 (s, 3H), 3.95 (q, 2H, J = 6.8 Hz), 4.15 (s, 2H), 6.75 (d, 1H, J = 8.3 Hz), 6.91 (m, 2H), 7.14 (t, 1H, J = 7.5 Hz); ^{13}C NMR ($CDCl_3$) δ 14.7, 27.8, 29.6, 30.5, 32.0, 63.5, 108.0, 114.1, 117.1, 123.2, 129.9, 134.7, 147.5, 149.5, 151.5, 155.2, 159.2; EI-HRMS m/z: calcd for $C_{17}H_{20}N_4O_3S$, 360.1256, found 360.1261.

4.3.8. 8-{[(4-Chlorophenyl)sulfanyl]methyl}caffeine (4h)

The title compound was prepared from 2-[(4-chlorophenyl)sulfanyl]acetic acid in a yield of 59%: mp 149–150 °C (methanol/ethylacetate 7:2). ^{1}H NMR ($CDCl_3$) δ, 3.34 (s, 3H), 3.46 (s, 3H), 3.86 (s, 3H), 4.12 (s, 2H), 7.23 (d, 2H, J = 7.5 Hz), 7.29 (d, 2H, J = 7.5 Hz); ^{13}C NMR ($CDCl_3$) δ; 27.9, 29.6, 30.8, 32.1, 108.0, 129.3, 131.8, 133.0, 134.1, 147.4, 149.0, 151.4, 155.2; EI-HRMS m/z: calcd for $C_{15}H_{15}ClN_4O_2S$, 350.0604, found 350.0597.

4.3.9. 8-{[(4-Bromophenyl)sulfanyl]methyl}caffeine (4i)

The title compound was prepared from 2-[(4-bromophenyl)sulfanyl]acetic acid in a yield of 73%: mp 160–164 °C (methanol/ethylacetate 7:2). ^{1}H NMR ($CDCl_3$) δ, 3.39 (s, 3H), 3.51 (s, 3H), 3.92 (s, 3H), 4.17 (s, 2H), 7.27 (d, 2H, J = 7.5 Hz), 7.42 (d, 2H, J = 7.5 Hz); ^{13}C NMR ($CDCl_3$) δ; 27.9, 29.6, 30.6, 32.1, 108.0, 122.1, 132.2, 132.5, 133.0, 147.4, 149.0, 151.4, 155.2; EI-HRMS m/z: calcd for $C_{15}H_{15}BrN_4O_2S$, 394.0099, found 394.0092.

4.4. Synthesis of 8-[(phenylsulfanyl)ethyl]caffeine derivatives (5a–e)

Compounds **5a**–**e** were synthesized from 1,3-dimethyl-5,6-diaminouracil[23] and an appropriate 3-(phenylsulfanyl)propanoic acid according to the procedure described above for the syntheses of **3a**–**j**.[22]

4.4.1. 8-[(Phenylsulfanyl)ethyl]caffeine (5a)

The title compound was prepared from 3-(phenylsulfanyl)propanoic acid in a yield of 45%: mp 143–145 °C (methanol/ethylacetate 7:2). ^{1}H NMR ($CDCl_3$) δ, 3.00 (t, 2H, J = 7.2 Hz), 3.35 (s, 3H), 3.35 (t, 2H, J = 7.2 Hz), 3.50 (s, 3H), 3.79 (s, 3H), 7.15 (m, 1H), 7.24 (m, 2H), 7.31 (m, 2H); ^{13}C NMR ($CDCl_3$) δ; 26.9, 27.8, 29.6, 31.7, 31.8, 107.3, 126.6, 129.0, 129.7, 134.7, 147.9, 151.6, 151.9, 155.2; EI-HRMS m/z: calcd for $C_{16}H_{18}N_4O_2S$, 330.1150, found 330.1148.

4.4.2. 8-{[(3-Chlorophenyl)sulfanyl]ethyl}caffeine (5b)

The title compound was prepared from 3-[(3-chlorophenyl)sulfanyl]propanoic acid in a yield of 3%: mp 181–183 °C (methanol/ethylacetate 7:2). ^{1}H NMR ($CDCl_3$) δ, 3.04 (t, 2H, J = 6.8 Hz), 3.37 (s, 3H), 3.39 (t, 2H, J = 6.8 Hz); 3.52 (s, 3H), 3.84 (s, 3H), 7.12 (m, 1H), 7.18 (m, 2H); 7.24 (m, 1H); ^{13}C NMR ($CDCl_3$) δ; 26.9, 27.8, 29.7, 31.6, 31.8, 107.3, 126.5, 127.4, 128.7, 130.0, 134.7, 137.0, 147.8, 151.5, 155.2; EI-HRMS m/z: calcd for $C_{16}H_{17}ClN_4O_2S$, 364.0761, found 364.0743.

4.4.3. 8-{[(3-Bromophenyl)sulfanyl]ethyl}caffeine (5c)

The title compound was prepared from 3-[(3-bromophenyl)sulfanyl]propanoic acid in a yield of 61%: mp 175–177 °C (methanol/ethylacetate 7:2). ^{1}H NMR ($CDCl_3$) δ, 2.90 (t, 2H, J = 6.4); 3.23 (s, 3H); 3.25 (t, 2H, J = 6.4 Hz); 3.38 (s, 3H), 3.70 (s, 3H), 6.97 (t, 1H, J = 7.5 Hz); 7.09 (d, 1H, J = 7.5 Hz); 7.13 (d, 1H, J = 6.8 Hz), 7.24 (s, 1H); ^{13}C NMR ($CDCl_3$) δ; 27.0, 27.8, 29.7, 31.7, 31.7, 107.3, 122.8, 127.9, 129.4, 130.2, 131.6, 137.3, 147.8, 151.5, 151.5, 155.1; EI-HRMS m/z: calcd for $C_{16}H_{17}BrN_4O_2S$, 408.0256, found 408.0255.

4.4.4. 8-{[(4-Chlorophenyl)sulfanyl]ethyl}caffeine (5d)

The title compound was prepared from 3-[(4-chlorophenyl)sulfanyl]propanoic acid in a yield of 23%: mp 148–150 °C (methanol/ethylacetate 7:2). ^{1}H NMR ($CDCl_3$) δ, 2.99 (t, 2H, J = 6.8 Hz); 3.34 (t, 2H, J = 6.8 Hz), 3.36 (s, 3H), 3.50 (s, 3H), 3.82 (s, 3H), 7.20 (d, 2H, J = 8.3 Hz); 7.23 (d, 2H, J = 8.3 Hz); ^{13}C NMR ($CDCl_3$) δ 26.9, 27.9, 29.6, 31.8, 32.1, 107.3, 129.1, 131.1, 132.7, 133.3, 147.9, 151.6, 151.6, 155.2; EI-HRMS m/z: calcd for $C_{16}H_{17}ClN_4O_2S$, 364.0761, found 364.0755.

4.4.5. 8-{[(4-Bromophenyl)sulfanyl]ethyl}caffeine (5e)

The title compound was prepared from 3-[(4-bromophenyl)sulfanyl]propanoic acid in a yield of 26%: mp 159–161 °C (methanol/ethylacetate 7:2). ^{1}H NMR ($CDCl_3$) δ, 3.00 (t, 2H, J = 6.8 Hz), 3.34 (t, 2H, J = 6.8 Hz), 3.35 (s, 3H), 3.49 (s, 3H), 3.81 (s, 3H), 7.15 (d, 2H, J = 8.3 Hz), 7.34 (d, 2H, J = 8.3 Hz); ^{13}C NMR ($CDCl_3$) δ 26.9, 27.8, 29.6, 31.7, 31.9, 107.2, 120.4, 131.2, 131.9, 133.9, 147.8, 151.5, 151.5, 155.2; EI-HRMS m/z: calcd for $C_{16}H_{17}BrN_4O_2S$, 408.0256, found 408.0255.

4.5. Synthesis of carboxylic acid derivatives (7, 9 and 10)

When not commercially available, the phenoxyacetic acids (**7**), 2-(phenylsulfanyl)acetic acids (**9**) and 3-(phenylsulfanyl)propanoic acids (**10**) required for the synthesis of **3–5** were synthesized according to literature procedures.[24,25] The experimentally determined as well as literature melting points of these acids are given in Table 1. The physical data of compound **9g**, previously unknown, is given below.

4.5.1. Phenoxyacetic acids (7)

An appropriately substituted phenol (50 mmol) was added to a solution of NaOH (187.5 mmol) in 15 mL of H_2O. Chloroacetic acid (85 mmol) was added slowly at to the resulting solution at 40 °C and the reaction mixture was heated to 85 °C. Stirring was continued for 2 h, the reaction was cooled to room temperature and 100 mL H_2O was added. The reaction was filtered and the filtrate was acidified with concentrated HCl to pH 1–2. The brown oil fraction which formed was extracted to diethylether (2 × 50 ml). The ether fraction, in turn, was extracted with an aqueous solution of 5% Na_2CO_3 (2 × 37.5 ml). The combined Na_2CO_3 fractions were acidified to pH 1–2 with concentrated HCl and the resulting precipitate was collected by filtration and oven dried to obtain the required acids.[24]

4.5.2. 2-(Phenylsulfanyl)acetic acids (9) and 3-(phenylsulfanyl)propanoic acids (10)

An appropriate thiophenol (10 mmol) was dissolved in ethanol (5 mL) and a solution of NaOH (10 mmol) in H_2O (3 mL) was added. In a separate flask, chloroacetic acid or 3-chloropropionic acid (11 mmol) was dissolved in H_2O (3 mL) and Na_2CO_3 (5.5 mmol) was added. The resulting solution was added to the thiophenol containing reaction and the reaction was allowed to stir at room temperature for 3 h. The reaction was subsequently heated under reflux for 1 h, cooled to room temperature and acidified with 2 N HCl to pH 2. H_2O (25 mL) was added and the brown oil fraction was extracted to diethylether (50 mL). The ether fraction was extracted with an aqueous solution of 5% Na_2CO_3 (25 ml). The Na_2CO_3 fraction was acidified to pH 2 with concentrated HCl and the resulting precipitate was collected by filtration and oven dried to obtain the required acids.[25] 2-[(3-Ethoxyphenyl)sulfanyl]acetic acid (**9g**): Yield 85%: mp 106 °C. ^{1}H NMR ($CDCl_3$) δ 1.38 (t, 3H, J = 7.2 Hz), 3.37 (s, 2H), 3.99 (q, 2H, J = 7.2 Hz), 6.75 (dd, 1H, J = 2.3, 8.3 Hz), 6.92–6.95 (m, 2H), 7.17 (t, 1H, J = 8.3 Hz); ^{13}C NMR ($CDCl_3$) δ 14.7, 36.2, 63.5, 113.6, 115.5, 121.6, 130.0, 135.6, 159.3, 174.3.

4.6. Determination of IC_{50} values

Microsomes from baculovirus infected insect cells expressing either recombinant human MAO-A or MAO-B (5 mg/mL) were obtained from Sigma–Aldrich, pre-aliquoted and stored at −70 °C. All enzymatic reactions were carried out to a final volume of 500 μL in 2 mL microcentrifuge tubes. Potassium phosphate buffer (100 mM, pH 7.4, made isotonic with KCl) served as reaction solvent.

4.6.1. IC_{50} measurements of 4a–i

The reactions contained the MAO-A/B mixed substrate, kynuramine (45 μM and 30 μM for MAO-A and -B, respectively), and various concentrations of the test inhibitor (0.003–100 μM). Stock solutions of the test inhibitors were prepared in DMSO and added to the reactions to yield a final concentration equal to 4% (v/v) DMSO. The reactions were initiated with the addition of MAO-A or -B (0.0075 mg/mL) and incubated at 37 °C for 20 min in a water bath. The reactions were subsequently terminated with the addition of 400 μL NaOH (2 N). After the addition of distilled water (1000 μL), the concentrations of the MAO generated 4-hydroxyquinoline were measured by fluorescence spectrophotometry (λ_{ex} = 310 nm, λ_{em} = 400 nm).[26] Quantitative estimations of 4-hydroxyquinoline concentrations were made via a linear calibration curve, which was constructed from solutions of 4-hydroxyquinoline (0.047–1.5 μM) in potassium phosphate buffer. To each standard solution (500 μL), 4% DMSO as co-solvent, 400 μL NaOH (2 N) and 1000 μL distilled water were added. The initial rate of kynuramine oxidation was graphed versus the logarithm of the inhibitor concentration to yield sigmoidal dose–response curves. For each curve, at least six different inhibitor concentrations spanning at least 3 orders of magnitude were used. The IC_{50} values were determined by fitting the sigmoidal curves to the one site competition model incorporated into the Prism 5 software package (GraphPad). All experiments were carried out in triplicate and the IC_{50} values are expressed as mean ± standard deviation (SD).[19]

4.6.2. IC_{50} measurements of 3a–j and 5a–e

The reactions contained kynuramine (45 μM and 30 μM for MAO-A and -B, respectively), various concentrations of the test inhibitor (0.003–100 μM), horseradish peroxidase (1 unit/mL) and Ampliflu Red (200 μM). Stock solutions of the test inhibitors were prepared in DMSO and added to the reactions to yield a final concentration of 4% (v/v) DMSO. The reactions were initiated with the addition of MAO-A or -B (0.0075 mg/mL), incubated at 37 °C for

20 min in a water bath and terminated with the addition of 10 μL (*R*)-deprenyl (5 mM) for MAO-B and 10 μL clorgyline (5 mM) for MAO-A. Distilled water (1400 μL) was added to each reaction and the concentrations of resorufin in the reactions were determined by fluorescence spectrophotometry (λ_{ex} = 560 nm, λ_{em} = 590 nm).[27] Quantitative estimations of resorufin were made by means of a linear calibration curve, which was constructed from solutions of H_2O_2 (0.05–1.6 μM). Each calibration standard was prepared to a final volume of 500 μL in potassium phosphate buffer and also contained horseradish peroxidase (1 unit/mL), Ampliflu Red (200 μM), 4% DMSO as co-solvent, 10 μL (*R*)-deprenyl (5 mM) for MAO-B and 10 μL clorgyline (5 mM) for MAO-A. Distilled water (1400 μL) was added to each standard. The IC_{50} values were determined as described above.

4.7. Time-dependence of inhibition

The time-dependencies of the inhibition of MAO-A and -B by selected inhibitors, compounds **3e** and **3c**, were examined. Recombinant human MAO-A and -B (0.03 mg/mL) were preincubated with compounds **3e** and **3c**, respectively for various periods of time (0, 15, 30, 60 min) at 37 °C. Potassium phosphate buffer (100 mM, pH 7.4, made isotonic with KCl) served as reaction solvent and the concentrations of inhibitors **3e** (9.7 μM) and **3c** (0.3 μM) were approximately twofold the measured IC_{50} value for the inhibition of MAO-A and -B, respectively. The preincubated reactions were subsequently diluted twofold by the addition of kynuramine to yield final kynuramine concentrations of 45 μM and 30 μM for MAO-A and -B, respectively. After dilution, the final concentrations of the **3e** and **3c** were approximately equal to the IC_{50} values and the final MAO concentration was 0.015 mg/mL. The reactions, which were carried out in 2 mL microcentrifuge tubes to a volume of 500 μL, were incubated for a further 15 min at 37 °C and terminated with the addition of 400 μL NaOH (2 N). After the addition of 1000 μL distilled water, the rates of the MAO generated of 4-hydroxyquinoline were measured spectrophotometrically as described above. All measurements were carried out in triplicate and are expressed as mean ± SD.[34,35]

4.8. Lineweaver–Burk plots

Since the caffeine derivatives examined here exhibit selective MAO-B inhibition, the mode of MAO-B inhibition by a selected inhibitor, compound **3c**, was investigated. For this inhibitor, a set consisting of 4 Lineweaver–Burk plots were constructed. One plot was constructed in the absence of inhibitor. To construct the remaining 3 plots, the concentrations selected for inhibitor **3c** were 0.0375–0.15 μM. Kynuramine at concentrations of 15–90 μM served as substrate and recombinant human MAO-B were used at a concentration of 0.015 mg/mL. The initial the rates of the MAO generated of 4-hydroxyquinoline were measured spectrophotometrically as described above. Linear regression analysis was performed using the Prism 5 software package.[34]

4.9. Molecular docking studies

Docking of selected inhibitors was accomplished with the Windows based Discovery Studio 3.1 software package (Accelrys Inc., San Diego, CA, USA).[29] The crystallographic models of MAO-A (PDB code, 2Z5X)[30] and MAO-B (PDB code, 2V60)[31] were acquired from the Brookhaven Protein Data Bank. The pK_a values and protonation states of the ionizable amino acids were calculated at pH 7.4 and hydrogen atoms were added accordingly to the models. When necessary, the valences of the FAD cofactors (oxidized state) and cocrystallized ligands were corrected and the enzyme models were typed with the Momany and Rone CHARMm forcefield. A fixed atom constraint was applied to the backbone of the enzyme models and the energies of the models were minimized using the Smart Minimizer protocol. For this purpose the maximum steps were set to 50000 and the implicit generalized Born solvation model with molecular volume was used. The cocrystallized ligands present in the active sites and the crystal water molecules were subsequently removed from the models and the binding sites were identified from the existing enzyme cavities. For the purpose of the docking procedure, the backbone constraint was also removed from the models. The following active site waters are considered conserved and were retained for the docking calculations: In the MAO-B active site, HOH 1159, 1166 and 1309 in the A-chain of 2V60.[31] In the MAO-A active site, HOH 710, 718 and 739 of 2Z5X. The structures of the selected inhibitors were constructed within Discovery Studio. Hydrogen atoms were added to the inhibitors and starting geometries of the structures were computed using a Dreiding-like forcefield (5000 iterations). Atom potential types and partial charges were assigned with the MMFF forcefield and the inhibitors were docked into the MAO models with the CDOCKER protocol. Allowance was made for the generation of 10 random ligand conformations, a heating target temperature of 700 K. The full potential was used for CDOCKER and in situ ligand minimization of the docking solutions was finally carried out using the Smart Minimizer algorithm. Unless otherwise specified, all the application modules within Discovery Studio were set to their default values. The illustrations were prepared with PyMOL.[36]

Acknowledgements

The NMR spectra were recorded by André Joubert of the SASOL Centre for Chemistry, North-West University while the MS spectra were recorded by Marelize Ferreira of the Mass Spectrometry Service, University of the Witwatersrand. This work was supported by grants from the National Research Foundation and the Medical Research Council, South Africa.

Supplementary data

Supplementary data associated with this article can be found, in the online version, at http://dx.doi.org/10.1016/j.bmc.2012.05.048.

References and notes

1. Youdim, M. B. H.; Bakhle, Y. S. *Br. J. Pharmacol.* **2006**, *147*, S287.
2. Edmondson, D. E.; Mattevi, A.; Binda, C.; Li, M.; Hubálek, F. *Curr. Med. Chem.* **2004**, *11*, 1983.
3. Binda, C.; Newton-Vinson, P.; Hubálek, F.; Edmondson, D. E.; Mattevi, A. *Nat. Struct. Biol.* **2002**, *9*, 22.
4. Youdim, M. B. H.; Edmondson, D.; Tipton, K. F. *Nat. Rev. Neurosci.* **2006**, *7*, 295.
5. Boulton, A. A. *Prog. Neuropsychopharmacol. Biol. Psychiatry* **1991**, *15*, 139.
6. Lasbennes, F.; Sercombe, R.; Seylaz, J. *J. Cereb. Blood Flow Metab.* **1983**, *3*, 521.
7. Da Prada, M.; Zürcher, G.; Würthrich, I.; Haefely, W. E. *J. Neural Tansm.* **1988**, *26*, 33.
8. Shih, J. C.; Chen, K.; Ridd, M. J. *Annu. Rev. Neurosci.* **1999**, *22*, 197.
9. Zisook, S. E. *Psychosomatics* **1985**, *26*, 240.
10. Birkmayer, W.; Riederer, P.; Ambrozi, L.; Youdim, M. B. *Lancet* **1977**, *309*, 439.
11. Finberg, J. P.; Wang, J.; Bankiewicz, K.; Harvey-White, J.; Kopin, I. J.; Goldstein, D. S. *J. Neural Transm. Suppl.* **1998**, *52*, 279.
12. Collins, G. G. S.; Sandler, M.; Williams, E. D.; Youdim, M. B. H. *Nature* **1970**, *225*, 817.
13. Kalaria, R. N.; Mitchell, M. J.; Harik, S. I. *Brain* **1988**, *111*, 1441.
14. Nicotra, A.; Pierucci, F.; Parvez, H.; Senatori, O. *Neurotoxicology* **2004**, *25*, 155.
15. Fowler, J. S.; Volkow, N. D.; Wang, G. J.; Logan, J.; Pappas, N.; Shea, C.; MacGregor, R. *Neurobiol. Aging* **1997**, *18*, 431.
16. Edmondson, D. E.; Binda, C.; Wang, J.; Upadhyay, A. K.; Mattevi, A. *Biochemistry* **2009**, *48*, 4220.
17. Menazza, S.; Blaauw, B.; Tiepolo, T.; Toniolo, L.; Braghetta, P.; Spolaore, B.; Reggiani, C.; Di Lisa, F.; Bonaldo, P.; Canton, M. *Hum. Mol. Genet.* **2010**, *19*, 4207.
18. Trouche, E.; Mias, C.; Seguelas, M. H.; Ordener, C.; Cussac, D.; Parini, A. *Stem Cells Dev.* **2010**, *19*, 1571.
19. Strydom, B.; Malan, S. F.; Castagnoli, N.; Bergh, J. J.; Petzer, J. P. *Bioorg. Med. Chem.* **2010**, *18*, 1018.

20. Booysen, H. P.; Moraal, C.; Terre'Blanche, G.; Petzer, A.; Bergh, J. J.; Petzer, J. P. *Bioorg. Med. Chem.* **2011**, *19*, 7507.
21. Di Monte, D. A.; DeLanney, L. E.; Irwin, I.; Royland, J. E.; Chan, P.; Jakowec, M. W.; Langston, J. W. *Brain Res.* **1996**, *738*, 53.
22. Suzuki, F.; Shimada, J.; Shiozaki, S.; Ichikawa, S.; Ishii, A.; Nakamura, J.; Nonaka, H.; Kobayashi, H.; Fuse, E. *J. Med. Chem.* **1993**, *36*, 2508.
23. Blicke, F. F.; Godt, H. C., Jr. *J. Am. Chem. Soc.* **1954**, *76*, 2798.
24. Zhao, G.; Yu, T.; Wang, R.; Wang, X.; Jing, Y. *Bioorg. Med. Chem.* **2005**, *13*, 4056.
25. Wang, T.; Zhang, Y.-H.; Kong, X.-W.; Lai, Y.-S.; Li, H.; Chen, Y.-P.; Peng, S.-X. *Chem. Biodivers.* **2009**, *6*, 466.
26. Novaroli, L.; Reist, M.; Favre, E.; Carotti, A.; Catto, M.; Carrupt, P. A. *Bioorg. Med. Chem.* **2005**, *13*, 6212.
27. Zhou, M.; Panchuk-Voloshina, N. *Anal. Biochem.* **1997**, *253*, 169.
28. Strydom, B.; Bergh, J. J.; Petzer, J. P. *Eur. J. Med. Chem.* **2011**, *46*, 3474.
29. http://accelrys.com/products/discovery-studio/.
30. Son, S.-Y.; Ma, J.; Kondou, Y.; Yoshimura, M.; Yamashita, E.; Tsukihara, T. *Proc. Natl. Acad. Sci. U.S.A.* **2008**, *105*, 5739.
31. Binda, C.; Wang, J.; Pisani, L.; Caccia, C.; Carotti, A.; Salvati, P.; Edmondson, D. E.; Mattevi, A. *J. Med. Chem.* **2007**, *50*, 5848.
32. Legoabe, L. J.; Petzer, A.; Petzer, J. P. *Eur. J. Med. Chem.* **2012**, *49*, 343.
33. Novaroli, L.; Daina, A.; Favre, E.; Bravo, J.; Carotti, A.; Leonetti, F.; Catto, M.; Carrupt, P. A.; Reist, M. *J. Med. Chem.* **2006**, *49*, 6264.
34. Manley-King, C. I.; Bergh, J. J.; Petzer, J. P. *Bioorg. Med. Chem.* **2011**, *19*, 261.
35. Petzer, A.; Harvey, B. H.; Wegener, G.; Petzer, J. P. *Toxicol. Appl. Pharm.* **2012**, *258*, 403.
36. DeLano, W. L. *The PyMOL Molecular Graphics System*; DeLano Scientific: San Carlos, USA, 2002.
37. Hayes, N. V.; Branch, G. E. K. *J. Am. Chem. Soc.* **1943**, *65*, 1555.
38. Newman, M.; Fones, W.; Renoll, M. *J. Am. Chem. Soc.* **1947**, *69*, 718.
39. Pasto, D. J.; McMillan, D.; Murphy, T. *J. Org. Chem.* **1965**, *30*, 2688.
40. Ahn, Y.; Cohen, T. *J. Org. Chem.* **1994**, *59*, 3142.
41. Degani, I.; Fochi, R.; Spunta, G. *Bollettino Scientifico della Facolta di Chimica Industriale di Bologna* **1966**, *24*, 75.